Simultaneous measurements of ion and electron currents using a novel compact electrostatic end-loss-current detector

M. Hirata, Y. Miyake, T. Cho, J. Kohagura, T. Numakura, K. Shimizu, M. Ito, S. Kiminami, N. Morimoto, K. Hirai, T. Yamagishi, Y. Miyata, Y. Nakashima, and S. Miyoshi
Plasma Research Centre, University of Tsukuba, Ibaraki 305-8577, Japan

K. Ogura
Graduate School of Science and Technology, Niigata University, Niigata 950-2181, Japan

T. Kondoh
Japan Atomic Energy Agency, Naka, Ibaraki 311-0193, Japan

T. Kariya
Toshiba Electron Tubes and Devices, Ohtawara, Tochigi 324-8550, Japan

(Received 8 May 2006; presented on 9 May 2006; accepted 25 July 2006; published online 13 October 2006)

For the purpose of end-loss-ion and -electron analyses in open-field plasmas, a compact-sized electrostatic end-loss-current detector is proposed on the basis of a self-collection principle for suppressing the effects of secondary-electron emission from a metal collector. For employing this specific method, it is worth noting that no further additional magnetic systems except the ambient open-ended magnetic fields are required in the detector operation. This characteristic property provides a compactness of the total detection system and availability for its use in plasma confinement devices without disturbing plasma-confining magnetic fields. The detector consists of a set of parallel metal plates with respect to lines of ambient magnetic forces of a plasma device for analyzing incident ion currents along with a grid for shielding the collector against strays due to the metal-plate biasing. The characterization experiments are carried out by the use of a test-ion-beam line along with an additional use of a Helmholtz coil system for the formation of open magnetic fields similar to those in the GAMMA 10 end region. The applications of the developed end-loss-current detector in the GAMMA 10 plasma experiments are demonstrated under the conditions with simultaneous incidence of energetic electrons produced by electron-cyclotron heatings for end-loss-plugging potential formation. © *2006 American Institute of Physics.*
[DOI: 10.1063/1.2338304]

I. INTRODUCTION

Ion diagnostics play various important roles in the studies of plasma parameters including ion currents, ion temperatures, plasma potentials, effects of radially sheared electric-field formation, and an ion-confinement time.[1–11] For the purpose of observations of these important parameters in tandem mirror plasmas, we have been developing several types of multigridded electrostatic ion-energy spectrometers[12–14] because of their compact-sized simple structures and convenient handling without the effects on the plasma-confining magnetic fields of the GAMMA 10 device.

Recently, the remarkable effects of radially produced shear of electric fields E_r on the suppression of turbulence-like fluctuations are found in the end-loss currents flowing from the central cell along with the central soft x-ray brightness.[15–22] The effects are observed in the form of remarkably different fluctuation levels and Fourier spectrum shapes in relation to the formation and disappearance of the vortexlike structures in the cases without and with E_r shears, respectively. To understand the common physics bases for such E_r shear confinement improvements, a remarkable characteristic advantage of open-ended mirror devices is employed. That is, a radial potential profile is easily controlled due to the axial electron flow produced by electron-cyclotron heatings (ECHs) from a plug ECH applied region.[1–6,23–27] The electrons flow into an end region along the lines of magnetic force. From this point of view, observations of the absolute values of the total ion and/or electron end-loss currents are of essential importance in order to identify confinement-time improvement as well as overall plasma confinement identification.

When detailed reproducibility of physically important phenomena during a plasma discharge is not expected, the simultaneous observations of various plasma parameters during a single plasma discharge are of significant importance for understanding the physics mechanisms. For this purpose, the present original detector is improved as follows. (1) A novel electrostatic absolute-value detector[28] is newly designed, in particular, for electron-current measurements. One of the improved points is to optimize the electrode size and shape to carry out ion- and electron-current measurements *simultaneously* by the use of this improved detector alone during a single plasma discharge (Fig. 1). This is made on the basis of computer simulation for their trajectories. (2)

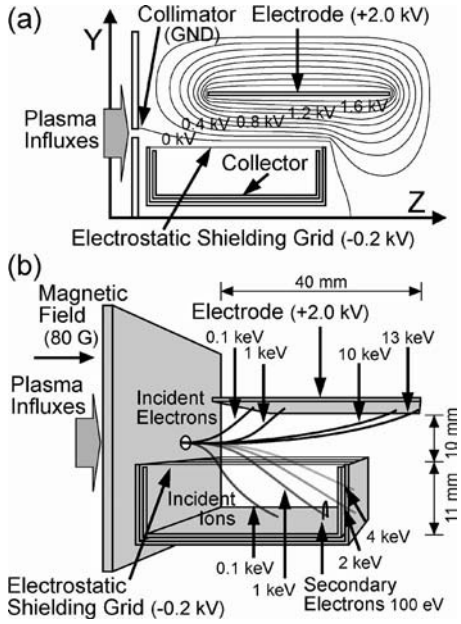

FIG. 1. (a) Schematic drawings of a novel compact end-loss-current detector and the calculation results of equipotential surfaces by the use of the finite element method. (b) Simulated trajectories for ions, electrons, and secondary electrons impinged from the metal collector hits by incident ion in the compact end-loss-current detector by the use of the Runge-Kutta method. The incident energies of ions and electrons are shown in (b). The secondary electron is automatically collected back due to the $\boldsymbol{E}\times\boldsymbol{B}$ drifts. Here, $\boldsymbol{B}=80$ G.

Bias voltages are also optimized for actual plasma experimental conditions due to incident ion- and electron-trajectory calculations (Fig. 1). (3) The validity of the new design and structure is confirmed and verified by characterization experiments by the use of a test-ion-beam line (Fig. 2). (4) This compact electrostatic end-loss-current detector is applied to measure the absolute values of ion and electron currents simultaneously in the GAMMA 10 tandem mirror experiments for the first time to attain plasma confinement time (see Sec. IV).

The above-described step-to-step improvements are reported in this article to verify the applicability of the present upgraded detector for both keV-order energetic bulk ion and electron diagnostics along the same line of sight for the only one detector with rather simple structure.

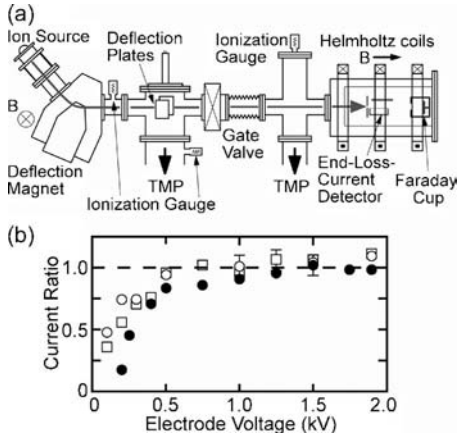

FIG. 2. (a) Schematic view of a monoenergetic ion-beam line for characterizing the novel compact end-loss-current detector. The Helmholtz coils are added for producing and mocking up open-ended fields for simulating the GAMMA 10 magnetic fields. (b) The ratio of observed currents from the collector to those from the Faraday cup is plotted as a function of the applied electrode voltage. The incident ions with the energies of 1 keV (open circles), 2 keV (open squares), and 3 keV (filled circles) are employed for the data plots.

II. A NOVEL COMPACT ELECTROSTATIC END-LOSS-CURRENT ABSOLUTE-VALUE DETECTOR

Figure 1(a) illustrates our developed novel compact-sized electrostatic end-loss-current detector. This detector is constructed with a set of parallely placed metal plates with respect to the lines of ambient magnetic force in an open-ended device along with a grid for shielding the collector against strays due to the metal-plate biasing. One of the plates is positively biased for separating incident ion and electron trajectories into another grounded metal-plate collector and positively biased plate due to the $\boldsymbol{E}\times\boldsymbol{B}$ drifts, respectively. The electrostatic shielding grid is constructed by stainless steel wire (0.03 mm in diameter) at 3 mm intervals in parallel with the lines of ambient magnetic forces. The ion transmission rate of the shielding grid is 99%. Also, the structure is proposed for giving no disturbances in ambient plasma-confining magnetic fields. No degradations in ion-current signals even under the conditions with simultaneous incidence of high-energy electrons produced by plug ECH.

In the case of +2 kV biased electrode, equipotential surfaces calculated by the finite element method are plotted at 200-V intervals in Fig. 1(a). Electric fields just behind the entrance are tailored and optimized by the use of −0.2 kV biased electrostatic shielding grid. Thereby, as one can see in Fig. 1(b), end-loss ions having wide variety in energies ranging from 100 eV to 4 keV in the GAMMA 10 experiments are sufficiently and completely collected. On the other hand, incident electrons in the energy range from 100 eV to 13 keV are bent to the electrode and completely collected. According to improvement in collector shape from flat plate to rectangular one as well as additional use of the electrostatic shielding grid, the enhancement of ion detection and the suppression of secondary electrons are realized.

III. CHARACTERIZATION EXPERIMENTS USING MONOENERGETIC ION-BEAM LINE WITH THE HELMHOLTZ COILS

For investigating the characteristic properties of the developed end-loss-current detector, a monoenergetic ion-beam line is employed [Fig. 2(a)]. An additional set of the Helmholtz coils is installed for producing and mocking up open-ended fields for simulating the GAMMA10 magnetic fields. The energy of the ion beam is varied by controlling the applied voltages. The incident monoenergetic ion beams are monitored and analyzed with a conventional Faraday cup.[11,12] The energy of the incident-ion beams, E_i, is confirmed with a recently developed electrostatic-ion-energy spectrometer. The energy dispersion ΔE_i of the incident beams is measured with a multigridded Faraday cup; its full

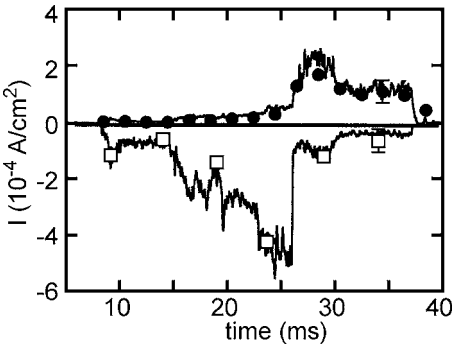

FIG. 3. The temporal evolution of end-loss-ion current densities in the positive regime and end-loss-electron current densities in the negative regime is plotted (see the solid curves) by means of the novel compact end-loss-current detector. End-loss-ion currents from the previously developed ion-energy-spectrometer (filled circles) and end-loss-electron currents from the multigridded Faraday cup (open squares) are also plotted for comparison.

width at half maximum (FWHM) value, limited by the flight length of the ion beams, is observed to be 25.0 eV at the peak value of E_i=1062.5 eV.

Hydrogen gas is utilized for an ion source to obtain similar situations to plasma experiments; the ion species of H^+, H_2^+, and H_3^+ are identified as a function of the coil currents for the bending magnet in the beam line, and H^+ is employed for the characterization experiments. The beam position is adjusted using electric fields produced by a set of parallel plates in the horizontal direction. The beam position in the vertical direction is adjusted with a bellows.

The novel end-loss-current detector is placed at the central position between the Helmholtz coil set. An 80 G magnetic-field intensity is generated by the Helmholtz coils for simulating the open-ended plasma-confining ambient magnetic fields at the detector location in GAMMA 10. The ratio of detection currents from the collector to those from the Faraday cup is plotted in Fig. 2(b) as a function of applied electrode voltage. Here, the Faraday cup is placed on the end-wall position of the end-loss-current detector for an ion-beam calibration use [see Fig. 2(a)].

The data in Fig. 2 are in good agreement on the values of the observed currents from the collector and the Faraday cup over the applied voltage of 1 kV. In the actual operation in GAMMA 10, 2 kV biasing is applied for the complete collection of incident electrons.

IV. AN APPLICATON OF THE COMPACT END-LOSS-CURRENT DETECTOR FOR PLASMA DIAGNOSTICS IN GAMMA 10

The novel end-loss-current detector [Fig. 1(a)] is utilized in GAMMA 10 for the observations of ions and electrons flowing along open-ended magnetic fields. Figure 3 shows the first data on the simultaneous measurements of end-loss-ion and -electron currents in the GAMMA 10 tandem mirror. Ion-current densities detected from the collector of the end-loss-current detector are presented in the positive region in Fig. 3. Electron-current densities detected from the electrode of the detector are also shown in the negative region in Fig. 3. During the ECH microwave injection (t=15–26 ms), the end-loss-electron currents increase for the formation of an ion-plugging potential in the plug region. After ECH is switched off, the end-loss-electron currents quickly decrease. However, end-loss-ion currents increase due to the quick disappearance of the ion-plugging potential for the suppression of the end-loss ions.

The observed data are compared to end-loss-ion currents from our previously developed obliquely placed multigridded ion-energy spectrometer (see filled circles in Fig. 3) and end-loss-electron currents detected from the multigridded Faraday cup established as electron energy spectrometer (open squares in Fig. 3). The ion- and electron-current densities denote good agreement with the conventional detector signals in Fig. 3. Reasonably behaved data confirm the applicability of the novel compact end-loss-current detector to the GAMMA 10 plasma experiments even under the conditions with the ECH applications.

Furthermore, the capability of an end-loss-current detector for simultaneous measurements of ion and electron current will also contribute to analyze not only a total particle-confinement time in the axial direction but also a radial transport effect according to comparison of each current fluctuation level (see Refs. 1–6).

[1] T. Cho *et al.*, Nucl. Fusion **45**, 1650 (2005).
[2] T. Cho *et al.*, Phys. Rev. Lett. **94**, 085002 (2005).
[3] M. Hirata *et al.*, Trans. Fusion Sci. Tech. **47**, 215 (2005).
[4] T. Cho *et al.*, Trans. Fusion Sci. Tech. **47**, 9 (2005).
[5] T. Cho *et al.*, J. Plasma Fusion Res. **80**, 81 (2004).
[6] T. Cho *et al.*, Nucl. Fusion **43**, 293 (2003).
[7] T. Cho *et al.*, Phys. Rev. Lett. **86**, 4310 (2001).
[8] T. Numakura *et al.*, Trans. Fusion Sci. Tech. **43**, 222 (2003).
[9] M. Hirata *et al.*, Nucl. Fusion **31**, 752 (1991).
[10] G. I. Dimov, J. Fusion Energy **19**, 87 (2001).
[11] T. Cho *et al.*, Nucl. Fusion **41**, 1161 (2001).
[12] Y. Sakamoto *et al.*, Rev. Sci. Instrum. **66**, 4928 (1995).
[13] M. Hirata *et al.*, Rev. Sci. Instrum. **74**, 1913 (2003).
[14] M. Hirata *et al.*, Trans. Fusion Technol. **39**, 281 (2001).
[15] T. Cho *et al.*, Nucl. Instrum. Methods Phys. Res. A **348**, 475 (1994).
[16] T. Cho *et al.*, Phys. Rev. A **46**, 3024 (1992).
[17] W. J. Price, *Nuclear Radiation Detection* (McGraw-Hill, New York, 1964).
[18] J. Kohagura *et al.*, Phys. Rev. E **56**, 5884 (1997).
[19] J. Kohagura *et al.*, Rev. Sci. Instrum. **66**, 2317 (1995).
[20] T. Numakura *et al.*, Plasma Phys. Controlled Fusion **45**, 807 (2003).
[21] M. Hirata *et al.*, Nucl. Instrum. Methods Phys. Res. A **477**, 210 (2002).
[22] M. Hirata *et al.*, Nucl. Instrum. Methods Phys. Res. B **66**, 479 (1992).
[23] T. Cho *et al.*, Phys. Rev. A **45**, 2532 (1992).
[24] T. Cho *et al.*, Phys. Rev. Lett. **64**, 1373 (1990).
[25] T. Cho *et al.*, Nucl. Fusion **28**, 2187 (1988).
[26] T. Cho *et al.*, Nucl. Fusion **27**, 1421 (1987).
[27] M. Hirata *et al.*, Rev. Sci. Instrum. **66**, 2311 (1995).
[28] M. Hirata *et al.*, Rev. Sci. Instrum. **75**, 3631 (2004).